

# CSIR South Africa mobile LIDAR—First scientific results: comparison with satellite, sun photometer and model simulations

V. Sivakumar<sup>a,b\*</sup>, M. Tesfaye<sup>a,b,c</sup>, W. Alemu<sup>a,c</sup>, D. Moema<sup>a,d</sup>, A. Sharma<sup>a</sup>, C. Bollig<sup>a</sup> and G. Mengistu<sup>c</sup>

**We present the first scientific results from the Council for Scientific and Industrial Research–National Laser Centre (CSIR-NLC) mobile Light Detection And Ranging (LIDAR) and its validation and comparison with other ground-based and space-borne measurements. The LIDAR results are compared with aerosol extinction measurements from the Stratosphere Aerosol Gas Experiment (SAGE) II, optical depth derived from sun photometers employed under the AEROSOL RObotic NETwork (AERONET) and backscatter coefficients simulated from weather balloon humidity measurements.**

**Key words:** AEROSOL, LIDAR measurements, optical depth, relative humidity

## 1. Introduction

Laser radar, more popularly known as LIDAR, uses electromagnetic radiation at optical frequencies. The radiation used by laser radars is at wavelengths which are 10 000 to 100 000 times shorter than those used by conventional radars. Backscattered photons reflected by the target are collected and processed to yield information about the target and/or the path to the target. Early conventional laser radars observed only the intensity of the collected radiation and the time delay from transmission to collection. Today, with technological advancements, LIDAR has become an excellent tool for monitoring the atmosphere in a relatively short period of time – a few seconds to minutes. Laser radars may incorporate continuous-wave or pulsed lasers which can either be focused or collimated. Continuous-wave laser radars are used when the signal may be integrated over long time periods and/or when the target is nearby. Pulsed laser radars, however, use much higher power levels, producing higher signal-to-noise ratios for the collected radiation. Generally, pulsed LIDARs are chosen for long-range remote sensing and when long signal integration is impractical. LIDAR systems are currently employed for studying the atmospheric structure and dynamics, trace constituents, aerosols, clouds, boundary and mixed layers, and other meteorological applications.

During the last 30 years, scientists have identified major aerosol types and they have developed general ideas about how the amount of aerosol varies in different seasons and locations. However, key details still are missing and we still have many unanswered questions about these tiny particles that are so fundamentally important to life on Earth and to understanding our climate; it is therefore crucial that scientists continue gathering relevant information (especially in southern hemisphere regions). In addition, optical and microphysical aerosol properties are currently considered as ‘low level’ within the climate change

scientific community although they are intricately involved in global warming.<sup>1</sup> In and around southern Africa, major cities produce large amounts of aerosols as a result of industrial activities and automobile emissions, in addition to natural biomass burning. In Saharan and northern Africa, volcanic eruptions and desert dust also contribute to aerosol concentrations.

Although ground-based LIDAR systems are deployed for atmospheric studies in many developed countries, it is still a very novel technique for South Africa and other African countries.<sup>2,3</sup> At present, there are only two LIDARs available in South Africa, located in Pretoria and Durban. Both LIDAR systems are similar in operation and specifications, which facilitates the establishment of simultaneous measurement studies. The Durban LIDAR<sup>4</sup> is operated at the University of KwaZulu-Natal as part of a collaboration between Réunion University and the Service d’Aéronomie (CNRS, IPSL, Paris) for climate research studies. The Council for Scientific and Industrial Research (CSIR)–National Laser Centre (NLC) in South Africa has recently designed and developed a mobile LIDAR system to contribute to atmospheric research in South Africa and other African countries.<sup>2</sup> The CSIR mobile LIDAR acts as an ideal tool to conduct measurements over southern hemisphere regions and encourages collaboration with other partners, who contribute to the space-borne and ground-based LIDAR measurements. At present, the system is capable of providing aerosol or cloud backscatter measurements for a height region from ground to 40 km with a 10 m vertical height resolution. The major advantage of the LIDAR is its ability to provide high resolution data capable of resolving structural details in the vertical cross-section of clouds, including cloud thickness, which is important for a better understanding of cloud dynamics and the earth-radiation budget.<sup>5</sup> This cloud information is also useful for predicting convective systems and rain. In general, LIDAR measurements will elucidate the aerosol concentration, optical depth, cloud position, thickness and other general properties of the cloud which are important for a better understanding of the earth-radiation budget, global climate change and turbulence.

In this paper, we present the first scientific results from the CSIR-NLC mobile LIDAR and its validation and/or comparison with other ground-based and space-borne measurements. In Section 2, we present a concise description of the CSIR-NLC mobile LIDAR (CNML) system. The description of the data and methods of analysis for determination of aerosol extinction profiles are outlined in Sections 3 and 4, respectively. The results and validation through other techniques and model simulations are presented in Section 5.

## 2. LIDAR system description

The LIDAR system comprises a laser transmitter, optical receiver and a data acquisition system. The complete LIDAR system is custom-fitted into a van using a shock absorber frame. Hydraulic stabiliser feet have been added to the vehicle suspension to

<sup>a</sup>National Laser Centre, Council for Scientific and Industrial Research, P.O. Box 395, Pretoria 0001, South Africa.

<sup>b</sup>Department of Geography, Geoinformatics and Meteorology, University of Pretoria, Lynnwood Road, Pretoria 0001, South Africa.

<sup>c</sup>Department of Physics, Addis Ababa University, Addis Ababa, Ethiopia.

<sup>d</sup>Tshwane University of Technology, Pretoria, South Africa.

\*Author for correspondence E-mail: svenkataraman@csir.co.za



Fig. 1. The CSIR-NLC mobile LIDAR system.

ensure stability during measurements (Fig. 1). A Nd:YAG laser is used for transmission, which is presently employed at the second harmonic (532 nm) at a repetition rate of 10 Hz.

The receiver system employs a Newtonian telescope configuration with a 406 mm (16 inch) diameter primary mirror. The backscattered signal is subjected to fall on the primary mirror of the telescope and is then focused toward a plane mirror kept at an angle of 45 degrees. The signal is detected by the photomultiplier tube (PMT) and the PMT output signal is transmitted to the transient digitiser and PC for analysis and archiving. A multimode optical fibre is used to couple the received backscatter optical signal from the telescope to the PMT. To accomplish accurate alignment of the fibre tip, a motorised 3D translation stage is used. The optical fibre is connected to an optical baffle which is positioned by the stage. The PMT is installed in an optical tube which converts the optical backscatter signal to an electronic signal which can be transferred to a PC for storage and analysis.

The data acquisition is performed by a transient recorder which communicates with a host computer for storage and offline processing of data. A Licel<sup>®</sup> transient digitiser is used, favoured for its capability for simultaneous analog and photon counting detection. This makes it highly suited to LIDAR applications by providing a high dynamic range. More details about the system are available in the literature.<sup>6</sup>

### 3. LIDAR and other datasets

#### LIDAR

The CNML has been operational since February 2008 and measurements have been made on an *ad hoc* basis during both day and night. As mentioned, collected data have a maximum altitude range of 40 km with a 10-m range resolution. In general, the received backscatter signals are averaged over 10 s to improve the signal-to-noise ratio (SNR). The data acquisition system has the capability of providing the backscatter signals simultaneously in analog and photon count forms. Obtained analog and photon count signals are appropriately glued in order to improve the signal strength and dynamic range. The LIDAR inversion technique is then applied to the glued data in order to obtain the aerosol backscatter and extinction coefficient. Measured aerosol backscatter and extinction coefficients were compared with other instruments to compare and validate the obtained results.

#### SAGE II

Stratospheric Aerosol and Gas Experiment II (SAGE II) was launched into orbit aboard the Earth Radiation Budget Satellite (ERBS) in October 1984.<sup>7</sup> During each sunrise and sunset encountered by the orbiting spacecraft, the instrument uses the solar occultation technique to measure attenuated solar radiation through the Earth's limb in seven channels centered at wavelengths ranging from 385 nm to 1 020 nm. The exo-atmospheric solar irradiance is also measured in each channel during each event, for use as a reference in determining limb transmittances. The transmittance measurements are inverted using the 'onion-peeling' approach to yield 1-km vertical resolution profiles of aerosol extinction (at 385 nm, 453 nm, 525 nm and 1 020 nm), ozone, nitrogen dioxide and water vapour.<sup>7,8</sup> The SAGE II instrument has collected vertical profiles of stratospheric and tropospheric aerosol extinction at four wavelengths with high resolution since the programme's inception in October 1984. We extracted the aerosol parameter, the aerosol extinction coefficients derived from version 6.20 series, of 21 years of data to characterise the aerosol climatology over Africa.

#### Sun photometer

The Aerosol Robotic Network (AERONET) (<http://www.aeronet.gsfc.nasa.gov>) provides a long-term, continuous and readily accessible public domain database of aerosol optical, microphysical and radiative properties for aerosol research and characterisation, validation of satellite retrievals, and synergism with other databases. Basically, it uses the sun photometer at different wavelengths to obtain aerosol properties, earth radiance and other physical properties. AERONET collaboration provides globally distributed observations of spectral aerosol optical depth (AOD), inversion products, and precipitable water in diverse aerosol regimes.<sup>9,10</sup> Here we used the aerosol optical thickness data (level 2) from Johannesburg, which have been validated with data obtained from the LIDAR and SAGE II.

#### Radiosonde

The radiosonde is a balloon-borne instrument capable of making direct *in situ* measurements of air temperature, humidity and pressure with height, typically to altitudes of approximately 30 km. The radiosonde transmits temperature and relative humidity data at each pressure level. The altitudes of these levels are calculated using the hydrostatic equation which relates the vertical height of a layer from the mean layer temperature, the humidity of the layer and the air pressure at the top and bottom of the layer. Here we used the radiosonde humidity data collected over Irene (near Pretoria) to simulate the aerosol backscatter coefficient through model calculations, based on the assumptions that aerosols are hygroscopic types and are water soluble. The quality of the Irene humidity data has been reported previously.<sup>11,12</sup>

### 4. Methods of analysis: LIDAR backscatter and extinction coefficient

The altitude profiles of aerosol extinction ( $\alpha$ ) or backscatter coefficient ( $\beta$ ) from a backscattered LIDAR signal require the solution for the LIDAR equation. The solution of the LIDAR equation is possible only if there is a relationship between these two unknown variables. Different inversion techniques are available depending on the relationship. Klett<sup>13</sup> assumed the following relationship between  $\beta$  and  $\alpha$ :

$$\beta = C\alpha k,$$

where  $C$  and  $k$  are constants.

This relationship is useful to solve the LIDAR equation in a highly turbid medium (scattering ratio >10). Generally, for a vertically pointing LIDAR which is used for upper tropospheric and stratospheric studies, this relationship is not applicable because  $C$  and  $k$  are variable with altitude, depending on the turbidity of the medium. The Klett<sup>13</sup> algorithm was later improved by considering the altitude variation of  $C$ .

For a monostatic single wavelength pulsed LIDAR system, the power received ( $P(z)$ ) from a range  $z$ , can be written as a single-scattering LIDAR equation:

$$P(z) = P_0 \frac{c\Delta t}{2} \frac{A}{z^2} \eta \beta(z) e^{-2 \int_0^z \alpha(z) dz}$$

where  $P_0$  is the transmitted power in watts,  $c$  is the speed of light,  $\Delta t$  is the laser pulse width,  $A$  is the area of the receiving mirror,  $\eta$  is the overall system efficiency,  $\beta(z)$  is the volume backscatter function = [ $\beta_a(z) + \beta_m(z)$ ], and  $\alpha(z)$  is the volume extinction function = [ $\alpha_a(z) + \alpha_m(z)$ ].

The  $\alpha_a$  and  $\beta_a$  are the volume extinction and backscatter coefficients of the aerosols and  $\alpha_m$  and  $\beta_m$  are the volume extinction and backscatter coefficients of the air molecules. The values of  $\alpha_m$  and  $\beta_m$  are calculated from the meteorological data or from a standard atmosphere model. Determinations of  $\alpha_a$  and  $\beta_a$  require an inversion of the LIDAR equation. The inversion is not a straightforward process since it involves two unknown variables. For this purpose, a definitive relationship between these two should be assumed. The molecular contributions to backscattering and extinction have been estimated using a reference model atmosphere (MSISE-90). This is accomplished by normalising the photon count with molecular density at a specified height (which varies from day to day), taken from a model (MSISE-90), and then applying the extinction correction to the backscattering coefficient profile using iterative analysis of the LIDAR inversion equation. The estimation of the aerosol backscatter coefficient applies the downward progression from the reference altitude of ~40 km where the aerosol concentration is said to be negligible.<sup>14</sup> The backscattering coefficient profiles, as computed above, are employed for the purpose of studying the cloud characteristics. For studying the aerosol concentrations, however, extinction profiles are computed following the LIDAR inversion method.<sup>15</sup>

**5. Results and discussion**

A sample height profile of the measured photon count is shown in Fig. 2. Here the signal represents the averaged photon count profiles for a period of 1 h, whereas the noise level is calculated based on the integrated signal over the upper height region from 38 km to 40 km, where we do not expect any aerosol concentrations. Subtracting the noise in such a way further reduces molecular concentrations in the profile. The integrated noise level is shown in Fig. 2, which distinguishes the signal for the height region at least up to 10 km. Above 10 km, the signal is found to be weaker, merely at the noise level, which is possibly due to the appearance of clouds at the height region of about 9 km. This cloud appearance would entirely prevent the laser beam from propagating upward any further, resulting in only noise being observed. On the other hand, during a clear day (no clouds or optically thin clouds), we are able to distinguish the signal even up to 35 km. Figure 2 clearly shows a sharp peak at approximately 9 km due to the passage of cloud over the site. The thickness of the cloud is found to be less than 500 m and this is a unique advantage of LIDAR, which is able to measure the cloud thickness which cannot be obtained from any other device

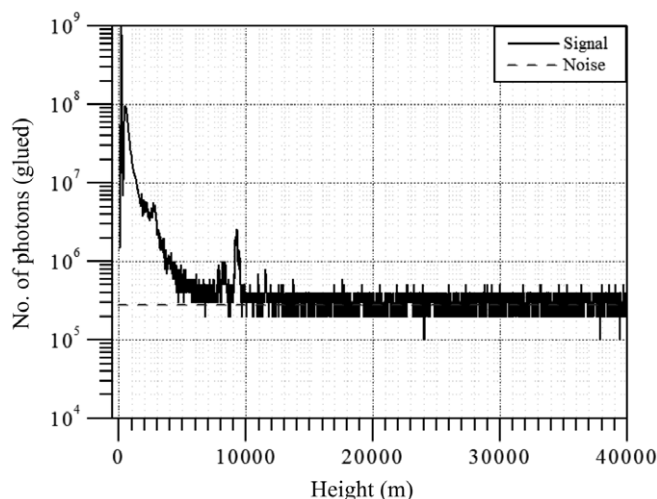


**Fig. 2.** Height profile of mean photon counts observed for 25 February 2008; the dotted line denotes the noise level.

or instrument. It is noted here that the present photon count profile stands for the measured data before the noise correction. In addition to the photon count profile, the data acquisition also simultaneously provides the analog signal information. One is able to integrate the analog and photon count profiles effectively to obtain the glued photon count information. The glued photon count profile further provides indicative information on aerosols, clouds etc., as it increases the dynamic range of the backscatter signal and improves the SNR. This has been explained in the literature.<sup>6</sup> It is briefly demonstrated in the following section using different signals. It should be noted here that the experiments were performed with two neutral density filters, in order to prevent PMT saturation and remove day-time background sunlight. Therefore the measured information was obtained from only 1% of the backscattered signal.

**Temporal evolution of LIDAR backscatter signal**

The temporal evolution of the backscattered LIDAR signal is plotted in Fig. 3, which illustrates the different forms of the signal— analog, photon count and glued photon count. Here, the glued photon count data refer to the merged analog and photon count signals after appropriately performing the scaling, dead time correction etc. The glued data greatly extend the dynamic range of detection. It is clear from Fig. 3 that the combined (glued) signal reveals a better picture of the structured atmosphere in comparison to the other two. It also is obvious that the analog signal does not show cloud structure whilst the photon count data illustrate a cloud picture over the upper height region. It is, however, noted that the analog form of the signal is more accurate for the lower height region in comparison to the upper height region. By combining the analog and photon count signals, the glued signal clearly reflects the presence of cloud on 25 February 2008 at around 10–12 km height regions (Fig. 3a). Such clouds are commonly referred to as cirrus clouds and are composed mostly of ice.<sup>16</sup>

The LIDAR also was operated during the night of 10 April 2008. The night was clear (no presence of cloud) and one would merely have expected aerosol backscattering. The temporal evolution of the aerosol structure is shown in Fig. 3b, which further evidences the planetary (nocturnal) boundary layer (PBL) structure. The PBL is found to be at approximately 3 km and is stable without much variation. During the night, when there is no solar input, aerosols are non-reactive and are found to be stable. During the day, however, the earth’s surface heats up

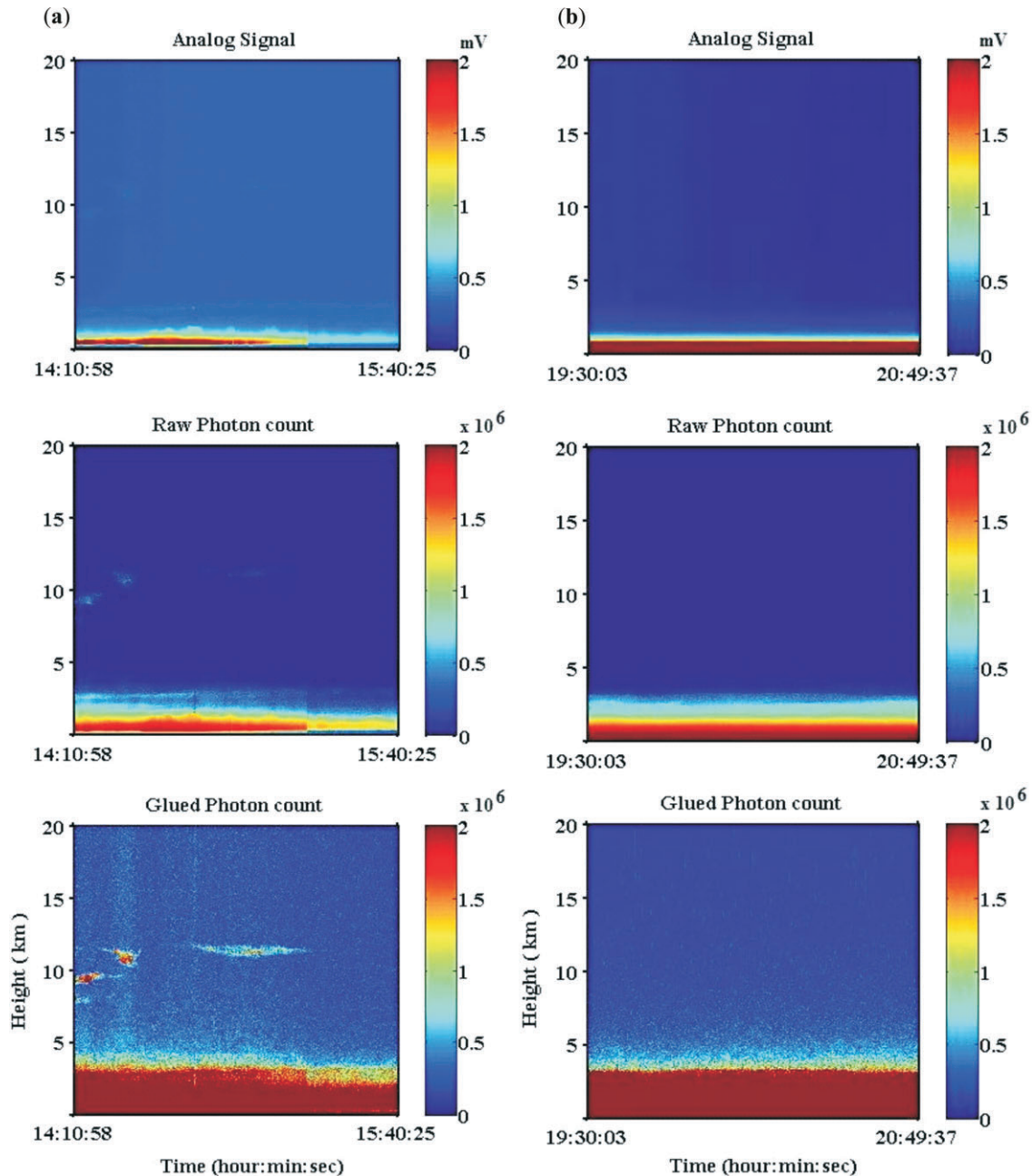


Fig. 3. Height-time-colour map of LIDAR signal returns for (a) 25 February 2008 and (b) 10 April 2008.

due to solar radiation and this results in various thermodynamic chemical reactions causing turbulence in the PBL. The boundary layer height is therefore expected to vary more during the day and to stabilise after sunset.

#### Aerosol extinction measurements by LIDAR and SAGE II

When validating the results from any instrument such as a LIDAR, accuracy is one of the most important criteria. Since the NLC mobile LIDAR is the first of its kind developed in South Africa for lower atmosphere studies, we have tried to validate the obtained results by comparing our measurements with those of space-borne and other ground-based data. As explained earlier in the data analysis, the SAGE II extinction profile at 525 nm was obtained over a southern African region (15°S to 40°S and 10°E to 40°E). The corresponding data for a period of approximately 20 years were downloaded from the NASA website ([http://eosweb.larc.nasa.gov/project/sage2/table\\_sage2.html](http://eosweb.larc.nasa.gov/project/sage2/table_sage2.html)). The SAGE II provides a height profile of aerosol extinction coeffi-

cient for the height region from 0.5 km to 40 km, which allowed comparison with the LIDAR measured aerosol extinction coefficient. We grouped the SAGE II profiles in terms of months to obtain the individual monthly mean aerosol extinction profiles for the height region from 0.5 km to 40 km. The corresponding monthly mean extinction profiles were compared with LIDAR data measured at 532 nm (with respect to the month of the date). Figure 4 illustrates the aerosol extinction coefficient derived from the SAGE II and LIDAR measured data obtained during the day on 25 February 2008 and the night of 10 April 2008. It is noted here that the LIDAR profiles are presented up to the height region where the SNR is found to be reasonable. It was found that both measurements were in good agreement, with less than 5% deviation. Such deviations are considered to be acceptable when comparing ground-based and space-borne measurements. Possible reasons for such deviations include: (a) the space-borne measurements being more accurate in the upper height regions while the ground-based data are more accurate at lower heights,

(b) the comparison being made between *monthly* mean extinction profiles, derived using 21 years of SAGE II satellite data over southern Africa, and LIDAR measurements on particular *days*, and (c) different operating modes used by the respective instruments—SAGE II uses solar occultation leading to horizontally average atmospheres while LIDAR measurements are obtained vertically. The minor differences in magnitude are expected to be within the standard deviations calculated from the long-term measurements. The values are in agreement with the extinction results obtained for the stratosphere height regions and those obtained using the LIDAR at the University of KwaZulu-Natal, Durban, where they also reported lower extinction values measured by LIDAR compared with those measured by SAGE II.<sup>4</sup> It is noted that SAGE II aerosol measurements are quite sensitive for the upper troposphere and stratosphere height regions in comparison to the lower troposphere. This is because the SAGE II sensor is not sensitive for the lower altitude. In addition, long-term LIDAR measurements are required to conclude the statement, including measurements over South African regions of interest (e.g. Highveld area) where we expect high variations in the aerosol extinction due to different levels of pollution. Our aim here was to compare the profiles in terms of approximate magnitudes between the LIDAR and satellite measurements.

On 10 April 2008, the LIDAR was operated during the night for approximately 2 h. The foggy background atmosphere resulted in the accumulation of aerosols (hygroscopic in nature), thereby allowing us to determine, and study, the boundary layer (~3 km). Assuming the hygroscopic nature of the aerosols, the aerosol backscatter coefficient was retrieved from the relative humidity measurement. The LIDAR-obtained aerosol extinction coefficients were closer to the SAGE II coefficients derived at 3 km and higher. LIDAR measurements were lower in comparison to the SAGE II climatological mean. The differences in sampling locations, measurement intervals and sampling years may have caused the deviations in extinction magnitude observed between LIDAR and SAGE II. However, the more recent SAGE III aerosol extinction measurements may provide more accurate results in comparison to those of SAGE II.<sup>8</sup>

The above LIDAR and SAGE II measurements were further used to obtain the integrated aerosol extinction coefficients for calculating the AOD. This is explained in detail in the following section. The mean aerosol extinction coefficient also was obtained over different regions (south, north, west and east) of Africa and will be further used in the future for comparison and validation of LIDAR results over Africa.

**Aerosol optical depth measurement and its comparison**

The aerosol extinction coefficients obtained using the LIDAR and SAGE II satellite data were integrated appropriately to get the height profile of aerosol extinction from the ground to 40 km.

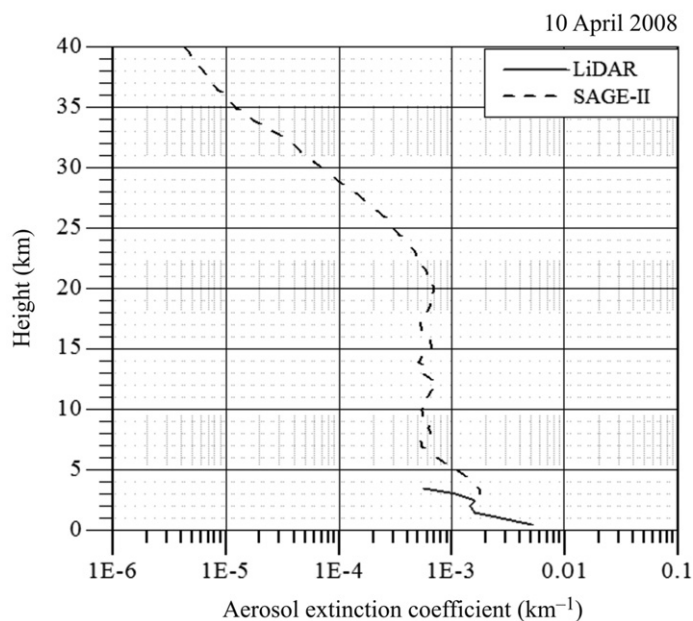


Fig. 4. Height profile of aerosol extinction coefficient retrieved from SAGE II and LIDAR.

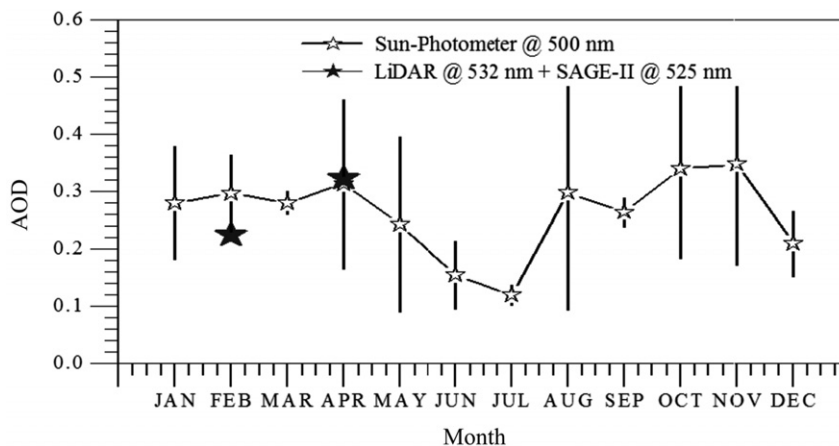


Fig. 5. Monthly climatology of aerosol optical depth (AOD) measurements derived from the sun photometer (mean ± s.d.) compared with the integrated LIDAR and SAGE II measurements.

Basically, the LIDAR-retrieved aerosol extinction is considered for the lower height region with respect to the SNR and at higher altitudes the extinction profile derived from the satellite is considered. We have considered the SAGE II profile as far as possible above 3–4 km, keeping in mind that the lower height region measurements are inaccurate due to low SNR.<sup>17</sup> The obtained extinction coefficient is integrated over height to obtain the optical depth over the particular site. The AERONET programme provides continuous optical depth information for Johannesburg (near to Pretoria) for approximately 8 years. Although Pretoria and Johannesburg are two different locations, our aim here was to approximate the magnitude of derived optical depth. Figure 5 illustrates the mean optical depth derived from the sun photometer wavelength centered at 500 nm. This depth has been compared with the AOD derived from LIDAR and SAGE II data. Here we have used quasi-continuous, monthly averaged aerosol extinction data (available from the website, <http://www.aeronet.gsfc.nasa.gov>) from ~6 years (May 2002 to August 2007). It is noted that there were months when no data were available (October 2002 to August 2005). The collected individual years of data were grouped in months, irrespective of the year, resulting in the calculated mean and standard

deviation for each respective month. Figure 5 indicates the mean AOD and the standard deviation obtained for the corresponding month. Since the wavelengths of the measurements are very close (500 nm from the sun photometer, 532 nm from the LIDAR and 525 nm from the SAGE II), we do not expect much deviation from the results. We calculated the optical depth from SAGE II and the LIDAR extinction profile for the corresponding two days (25 February 2008 and 10 April 2008) and compared these with the monthly climatological values. It is evident from Fig. 5 that the LIDAR- and SAGE II-derived optical depths are within the monthly variations obtained from the sun photometer. It is understood that small discrepancies in the magnitude may be due to different reasons, such as the type of instrument used, place of operation and the time period of measurements. Furthermore, SAGE II measurements are based on the limb occultation technique, which might raise the aerosol contribution over horizontal distances. In our calculations, this was considered as being negligible. In the near future, we plan to simultaneously operate the LIDAR in unison with the sun photometer measurements.

Figure 5 also illustrates that the value of the AOD has a strong seasonal dependence: maximum during late spring (October and November) and minimum during winter (May–July). The observed maximum during spring might be due to dust transport and biomass burning. This peak is in agreement with results obtained from Skukuza (in the north of South Africa) and has been interpreted to be a result of dust<sup>19</sup> from biomass burning<sup>18</sup> in China. The drop in AOD during December might be due to summer rainfall, similar to the result from the Indian Ocean Experiment (INDOEX).<sup>20</sup> The observed minimum AOD during winter is in agreement with the report from China;<sup>21</sup> they attributed the minimum value to snowfall in winter, which results in dust not being lifted upward into the atmosphere.

#### Aerosol backscatter coefficient measured by LIDAR and radiosonde

It is known that aerosol formations and sizes vary with respect to hygroscopic parameters<sup>22</sup> (e.g. relative humidity). An increase in relative humidity condenses the water vapour, causing aerosol formations which differ in their scattering behaviour depending on their chemical composition.<sup>23</sup> There is also a reduction in atmosphere visibility.<sup>22</sup> This phenomenon leads to an increase in the size of the particles (hygroscopic growth of aerosols) to significantly larger sizes when dry. A simple model calculation is proposed based on the assumption that the hygroscopic aerosols are dependent on the relative humidity.<sup>22,24,25</sup> The model parameterises the scatter-grown factors to assess the hygroscopic effect on aerosol backscatter. The normalised backscattering coefficients can be calculated by taking the ratio of aerosol backscatter over the mean backscatter observed for a reference

$$\text{relative humidity} \left( \frac{\beta^a(\lambda, r)}{\beta_{\text{ref}}^a(\lambda, r)} \right), \text{ where } \left( \frac{\beta^a(\lambda, r)}{\beta_{\text{ref}}^a(\lambda, r)} \right) = a \left( 1 - \frac{\text{Rh}}{100} \right)^{-b}.$$

Here  $\beta_{\text{ref}}^a(\lambda, r)$  is assumed at a relative humidity (Rh) value of 70%. It is found, based on the observational data and Rheinstein numerical results, that the reference  $\beta_{\text{ref}}^a(\lambda, r)$  for water-coated spherical aerosol backscattering is  $0.0005 \text{ km sr}^{-1}$ . The other two constants,  $a$  and  $b$ , are based on the numerical best fit to the data (in a least square sense and trial-error method) and yields values of  $a = 0.43$  and  $b = 0.3$ , with a regression coefficient of  $R^2 = 0.85$ .

Based on the radiosonde relative humidity measurements, we calculated the aerosol backscatter coefficients and compared them with those derived from the direct LIDAR backscatter measurements. Figure 6 shows the backscatter coefficients derived

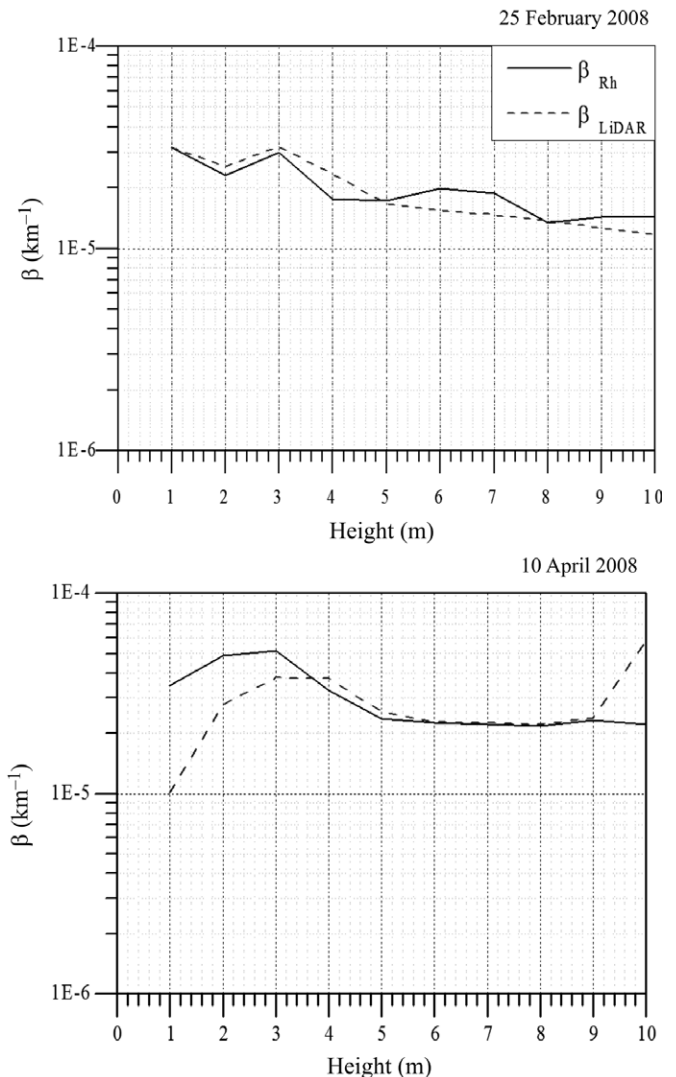


Fig. 6. Height profiles of aerosol backscatter coefficient measurements retrieved from the LIDAR and model simulation.

for the two different days, 25 February 2008 and 10 April 2008. On 25 February 2008, both measurements were in close agreement with each other up to 10 km. Above 10 km, the LIDAR measurements were questionable due to the presence of high, dense (cirrus) clouds. On 10 April 2008, the background atmosphere condition was foggy and favourable for aerosol growth. Although there was low agreement below 4 km, the measured and simulated backscatter coefficients were found to be in good agreement between 4 km and 9 km. The observed difference in the magnitudes may be attributed to one dataset using model-simulated data and the other using measured LIDAR data. The contribution of non-hygroscopic aerosols and theoretical model approximations may also contribute to the underestimation of the backscatter coefficient. In general, the results are in good agreement and this further addresses the possibility for classifying aerosols into hygroscopic and non-hygroscopic species. Based on the temperature information (from radiosonde measurements), we found that the disagreement between the simulated and measured LIDAR data arises when the temperature falls below  $0^\circ\text{C}$  (data not shown).

#### 6. Summary and future perspectives

We have presented the first scientific results from the CSIR-NLC mobile LIDAR and its validation and/or comparison

with other ground-based and space-borne measurements. The LIDAR results were validated against SAGE measurements, optical depths derived from a sun photometer employed under AERONET, and model-simulated backscatter coefficients based on relative humidity measurements from radiosonde. The agreements were found to be reasonable and indicate the accuracy of the LIDAR measurements. It is clear from the comparison that LIDAR measurements provide high vertical resolution data and this permits us to study the atmosphere structure in comparison to the SAGE or AERONET datasets. Our future plans include field measurements at different sites in South Africa and improvements in the system to enable making 2D and water vapour measurements.

The LIDAR project team is thankful to numerous colleagues at the National Laser Centre for their help. The authors are also grateful to the different South African funding agencies: Council for Scientific and Industrial Research–National Laser Centre (CSIR-NLC), Department of Science and Technology (DST), National Research Foundation (NRF) (Grant no: 65086) and the African Laser Centre (ALC). We also express our thanks to SAGE II, AERONET and radiosonde data centres for providing access to the required data.

Received 1 June. Accepted 4 September 2009.

- IPCC Climate Change (2007). The Physical Science Basis. In *Contribution of Working Group I to the Fourth Assessment Report of the Intergovernmental Panel on Climate Change*, eds S. Solomon, D. Qin, M. Manning, Z. Chen, M. Marquis, K.B. Averyt, M. Tignor and H.L. Miller. Cambridge University Press, Cambridge & New York.
- Sivakumar V., Moema D., Sharma A., Mbatha N., Bollig C., Malinga S., Mengistu G., Bencherif H. and Keckhut P. (2008). LIDAR for atmosphere research over Africa – a trilateral research programme (LARA – trip). In *Proceedings of the 24th International Laser Radar Conference, Boulder, USA*, pp. 742–745. University of Colorado, Boulder.
- Sivakumar V. (2008). *Lidar Research in South Africa*. The International Society for Optical Engineering (SPIE), Invited news room article, doi 10.1117/2.1200808.1250.
- Moorgawa A., Bencherif H., Michaelis M.M., Porteneuve J. and Malinga S. (2007). The Durban atmospheric LIDAR. *Optics Laser Technol.* **39**, 306–312.
- Michal S., Zelinger Z., Sivakumar V. and Engst P. (2008). Lidar for ground- and airborne trace gas detection. In *Lasers in Chemistry*, vol. 1, ed. M. Lackner, chap. 6, pp. 131–171. Wiley-VCH, Weinheim.
- Sivakumar V., Sharma A., Moema D., Bollig C., van der Westhuizen C. and van Wyk H. (2008). CSIR-NLC South Africa Mobile LIDAR system description. In *Proceedings of the 24th International Laser Radar Conference, Boulder, USA*, pp. 99–102. University of Colorado, Boulder.
- Chu W., McCormick M., Lenoble J., Brogniez C. and Pruvost P. (1989). SAGE II inversion algorithm. *J. Geophys. Res.* **94**, 8339–8351.
- Thomason L., Poole L. and Randall C. (2007). SAGE III aerosol extinction validation in the Arctic winter: comparisons with SAGE II and POAM III. *Atmos. Chem. Phys.* **7**, 1423–1433.
- Holben B.N., Eck T.F., Slutsker I., Tanre D., Buis J.P., Setzer A., Vermote E., Reagan J.A., Kaufman Y.J., Nakajima T., Lavenue F., Jankowiak I. and Smimov A. (1998). AERONET – a federated instrument network and data archive for aerosol characterization. *Rem. Sens. Environ.* **66**, 1–16.
- Holben B.N., Tanre D., Smirnov A., Eck T.F., Slutsker I., Abuhassen N., Newcomb W.W., Schafer J., Chatenet B., Lavenue F., Kaufman Y.J., Vande Castle J., Setzer A., Markham B., Clark D., Frouin R., Halthore R., Karnieli A., O'Neill N.T., Pietras C., Pinker R.T., Voss K. and Zibordi G. (2001). An emerging ground-based aerosol climatology: aerosol optical depth from AERONET. *J. Geophys. Res.* **106**, 12067–12097.
- Sivakumar V., Tefera D., Mengistu G. and Botai O.J. (In press). Mean ozone and water vapour height profiles for southern hemisphere region using Radiosonde/Ozonesonde and HALOE satellite data. *Adv. Geosci.*
- Botai O.J., Sivakumar V., Combrinck L.W. and Hannes C.J. (In press). Multi-scale organisation of water vapour in the low- and mid-tropical Africa. *Adv. Geosci.*
- Klett J.D. (1981). Stable analytical inversion solution for processing LIDAR returns. *Appl. Opt.* **20**, 211.
- Bencherif H., Portafaix T., Baray J.L., Morel B., Baldy S., Leveau J., Moorgawa A., Michaelis M., Hauchecorne A., Keckhut P. and Diab R. (2003). LIDAR observations of lower stratospheric aerosols over South Africa linked to large scale transport across the southern subtropical barrier. *J. Atmos. Solar-Terr. Phys.* **65**, 707–715.
- Klett J.D. (1985). Lidar inversion with variable backscatter to extinction ratios. *Appl. Opt.* **24**, 1638–1645.
- Sivakumar V., Bhavanikumar Y., Rao P.B., Mizutani K., Aoki T., Yasui M. and Itabe T. (2003). Lidar observed characteristics of tropical cirrus clouds. *Radio Sci.* **38**(6), 1094.
- Randall C.E., Bevilacqua R.M., Lumpe J.D. and Hoppel K.W. (2001). Validation of POAM III aerosols: comparison to SAGE II and HALOE. *J. Geophys. Res.* **106**(D21), 27525–27536.
- Formenti P., Winkler H., Fourie P., Piketh S., Makgopa B., Helas G. and Andreae M.O. (2002). Aerosol optical depth over remote semi arid region of South Africa from spectral measurements of the daytime solar extinction and night-time stellar extinction. *Atmos. Res.* **62**, 11–32.
- Gai C., Li X. and Zhao F. (2006). Mineral properties observed in north west region of China. *Glob. Planet. Change* **52**, 173–181.
- Pillai P.S., Jhurry D. and Moorthy K.K. (2001). Aerosol optical depth studies during INDOEX: comparison of the spectral features over coastal India with pristine southern hemispheric environment over Mauritius. *Curr. Sci. (Suppl.)* **80**, 2001.
- Niu S. and Xu X. (2008). Dust aerosol optical properties over North China. *Atmos. Chem. Phys. Discuss.* **8**, 17037–17059.
- Randriamiarisoa H., Chazette P., Couvert P., Sanak J. and M'egie G. (2006). Relative humidity impact on aerosol parameters in a Paris suburban area. *Atmos. Chem. Phys.* **6**, 1389–1407.
- Tang I.N. and Munkelwitz H.R. (1993). Composition and temperature dependence of the deliquescence properties of hygroscopic aerosols. *Atmos. Environ.* **27A**, 467–473.
- Hanel G. (1976). The properties of atmospheric aerosol particles as functions of the relative humidity at thermodynamic equilibrium with the surrounding moist air. *Adv. Geophys.* **19**, 73–188.
- Covert D.S., Charlson R.J. and Ahlquist N.C. (1972). A study of the relationship of chemical composition and humidity to light scattering by aerosols. *J. Appl. Meteorol.* **11**, 968–976.